# Comparative proteomic analysis of irinotecan-sensitive colorectal carcinoma cell line and its chemoresistant counterpart

Feng-Ming Gong, Xing-Chen Peng, Ben-Xu Tan, Jun Ge, Xi Chen, Ye Chen, Feng Xu, Feng Bi, Jian-Mei Hou and Ji-Yan Liu

**In this study, we used two-dimensional gel electrophoresis and MALDI-Q-TOF-MS/MS analysis to examine the global protein expression of a pair of colorectal carcinoma cell lines, SW620 and irinotecan-resistant SW620. Of the 30 spots identified as differentially expressed proteins (± over twofold, $P < 0.05$) between the two cell lines, 26 spots (corresponding to 26 unique proteins) were positively identified by MALDI-Q-TOF-MS/MS analysis. These proteins could be grouped into main classes including metabolism (15.38%), cell SSproliferation/ differentiation (11.53%), molecular chaperone (11.53%), mRNA splicing (11.53%), and so on. The proteins, which might be involved in the development of tumor drug resistance, such as α-enolase, cofilin, and thioredoxin-dependent peroxide 1, have been validated by western blot analysis and have been discussed. The proteins identified in this study may be useful in showing the mechanisms underlying irinotecan resistance.** ***Anti-Cancer Drugs*** **22:500–506 © 2011 Wolters Kluwer Health | Lippincott Williams & Wilkins.**

**Anti-Cancer Drugs** 2011, **22**:500–506

**Keywords: colorectal carcinoma, drug resistance, irinotecan, two-dimensional gel electrophoresis**

Department of Medical Oncology, Cancer Center, the State Key Laboratory of Biotherapy, West China Hospital, West China Medical School, Sichuan University, No. 37, Guo Xue Xiang, Chengdu, Sichuan Province

Correspondence to Dr Ji-Yan Liu, Department of Medical Oncology, Cancer Center, the State Key Laboratory of Biotherapy, West China Hospital, West China Medical School, Sichuan University, No. 37, Guo Xue Xiang, Chengdu, The People's Republic of China
Tel: +86 28 85423262; fax: +86 28 85423609;
e-mail: liujiyan1972@163.com

Feng-Ming Gong and Xing-Chen Peng contributed equally to this study

**Received** 25 May 2010 **Revised form accepted** 14 September 2010

## Introduction

Colorectal carcinoma (CRC) is one of the most frequent malignancies and is associated with a high mortality rate [1]. In 2008, 150 000 new CRC cases and over 50 000 deaths because of CRC were estimated in the USA [2]. The mainstay of nonsurgical treatment for advanced CRC has been 5-fluorouracil, combined with irinotecan or oxaliplatin [3,4]. Irinotecan is a chemotherapeutic agent that causes S-phase-specific cell killing by poisoning topoisomerase I in the cells [5]. However, frequent acquisition of irinotecan chemotherapy resistance partly accounts for the poor therapy outcome of this cancer. Several mechanisms were involved in the development of acquired irinotecan resistance, such as low carboxylesterase expression [6], overexpression of UDT-glucuronosyltranferase at the protein and mRNA levels [7], overexpression of P-glycoprotein and multidrug resistance associated protein (MRP) [8], irinotecan-induced DNA damage [9], NF-κB activation [10], and so on. Although these mechanisms partly interpreted irinotecan-induced chemoresistance, additional factors may play an important role in promoting resistance to irinotecan. The other underlying mechanisms are worthy of investigation.

Proteomic techniques are ideal methods to study the global changes in protein expression, especially those involved in the chemotherapy resistance [11,12]. To increase the understanding of the mechanisms involved in the irinotecan resistance, the protein expression profiles of two human CRC cell lines: SW620 and irinotecan-resistant SW620 (SW620/irinotecan), were analyzed by two-dimensional gel electrophoresis (2-DE) and MALDI-Q-TOF-MS/MS. Proteins of interest were excised and subjected to microsequencing analysis. Twenty-six proteins, which were present in different quantities in these two cell lines, were identified. Western blot analysis showed that the expression levels of thioredoxin-dependent peroxide 1 (TDPX1), α-enolase, and cofilin were obviously altered. We believe that such identified proteins may improve the understanding of the mechanisms leading to the acquisition of irinotecan chemoresistance.

## Materials and methods

### Cell culture and sample preparation

SW620 (ATCC, Rockville, Maryland, USA) cells were maintained in Dulbecco modified Eagle medium (Gibco, USA) containing 10% fetal calf serum (Hyclone, USA), penicillin (100 U/ml), and streptomycin (10 mg/l) at 37°C in an atmosphere containing 5% carbon dioxide. The chemoresistant cell line named SW620/irinotecan was selected from the wild-type SW620 cell line by chronic exposure to irinotecan (Sigma Chemical Co., St. Louis, Missouri, USA) at intermittent dosage schedules at sufficient intervals to permit the expression of the

0959-4973 © 2011 Wolters Kluwer Health | Lippincott Williams & Wilkins DOI: 10.1097/CAD.0b013e3283408596

resistance phenotypes. The cells were exposed to the drug starting from $1 \times IC_{50}$, and the drug concentrations were escalated at an increasing rate of 50%. The cells were finally cultured in the medium with a concentration of ten times higher than $1 \times IC_{50}$. The chemoresistant cell line was established and subcultured twice per week for more than 6 months until stable cell lines were established. For the 2-DE analysis, the cells (80% confluence) were washed twice with PBS before harvesting. The cells were stored at $-80^{\circ}C$ until use.

#### Drug sensitivity assay

The cultured cells were suspended in Dulbecco modified Eagle medium at $1 \times 10^5$ cells/ml. A sample of 100 µl of the cell suspension was seeded into a 96-well plate. After an overnight culture, the cells were exposed to irinotecan for 48 h. After incubation with 3-(4, 5-dimethylthiazol-2-yl)-2, 5-diphenyltetrazolium bromide (0.5 mg/ml) for 4 h, the medium was removed and 150 µl of dimethylsulfoxide was added to dissolve formazan crystals. Absorbance was measured at 490 nm using an ELISA microplate reader (PerkinElmer, Wellesley, Massachusetts, USA). Cell survival rates were calculated according to the formula: survival rate = (mean OD of treated wells/mean OD of untreated wells) × 100%. Finally, dose-effect curves of anti-cancer drugs were drawn on a semilogarithm coordinate paper and $IC_{50}$ values were determined.

#### Two-dimensional gel electrophoresis and image analysis

Approximately $2 \times 10^7$ cells were lysed in 0.5 ml of lysis buffer (7 mol/l urea, 2 mol/l thiourea, 4% CHAPS, 100 mmol/l dithiothreitol, 0.2% pH 3–10 ampholyte; Bio-Rad, USA) containing the protease inhibitor cocktail 8340 (Sigma, St. Louis, Missouri, USA). Samples were then kept on ice and sonicated in six cycles for 15 s, each consisting of 5-s sonication followed by a 10-s break. After centrifugation at 15 000 rpm for 1 h at 4°C, the supernatant was collected and the protein concentrations were determined using the DC protein assay kit (Bio-Rad). Protein samples (2 mg) were applied to an immobilized pH gradient strip (17 cm, pH3–10NL; Bio-Rad) using a passive rehydration method. After 12–16 h of rehydration, the strips were transferred to an IEF Cell (Bio-Rad). Isoelectric focusing (IEF) was performed as follows: 250 V for 30 min, linear; 1000 V for 1 h, rapid; linear ramping to 10 000 V for 5 h, and finally 10 000 V for 5 h [13]. The second dimension was performed using 12% SDS-PAGE at 30 mA constant current per gel after equilibration [14]. The gels were stained using CBB R-250 (Merck, Germany) and scanned with a molecular imager GS-800 USB calibrated densitometer scanner (Bio-Rad). Four independent runs were made for each cell line to ensure the accuracy of the analyses. The maps were analyzed using the PDQuest Software Version 6.1 (Bio-Rad). The quantity of each spot in a gel was normalized as a percentage of the total quantity of all spots in that gel and evaluated in terms of OD. For statistical analysis, the paired *t*-test was carried out to compare data from the four repeated experiments. Only spots that showed significant differences ( ± over two-fold, $P < 0.05$) were selected for analysis by mass spectroscopy (MS).

#### In-gel digestion

In-gel digestion of proteins was carried out using MS-grade Trypsin Gold (Promega, Madison, Wisconsin, USA) according to the manufacturer's instructions. In brief, spots were cut out of the gel (1–2 mm diameter) using a razor blade and destained twice with 100 mmol/l $NH_4HCO_3$/50% acetonitrile at 37°C for 45 min, in each treatment. After drying, the gels were preincubated in 10–20 µl trypsin solution for 1 h. Then, 15-µl digestion buffer was added (40 mmol/l $NH_4HCO_3$/10% acetonitrile) to cover each gel and incubated overnight at 37°C. Tryptic digests were extracted using MilliQ water initially, followed by twice extraction with 50% acetonitrile/5% trifluoroacetic acid for 1 h each time. The combined extracts were dried in a vacuum concentrator at room temperature. The samples were then subjected to MS analysis [13,14].

#### Tandem mass spectroscopy analysis and protein identification

Mass spectra were acquired using a Q-TOF mass spectrometer (Micromass, Manchester, UK) fitted with an ESI or MALDI source (Micromass). MALDI-Q-TOF analysis was carried out as described earlier [13]. As for the MALDI-Q-TOF analysis, the automatic scan rate was 1.0 s with an interscan delay of 0.02 s, and the system was operated at 3.0 kV. Spectra were accumulated until a satisfactory S/N had been obtained. Parent mass peaks with the range from 400 to 1600 m/z were picked out for tandem mass spectroscopy (MS/MS) analysis. The collision energy was chosen to vary between 18 and 57 eV depending on the mass of the precursor. The MS/MS data were acquired and processed using the MassLynx V 4.1 Software (Micromass) and were converted to PKL files by the ProteinLynx 2.2.5 Software (Waters, Massachusetts, USA). The PKL files were analyzed using the MASCOT search engine (*http://www.matrixscience.com*). The search parameters were defined as follows: database, Swiss-Prot; taxonomy, *Homo sapiens*; enzyme, trypsin, and allowance of one missed cleavage. Carbamidomethylation was selected as a fixed modification and oxidation of methionine was allowed to be variable. The peptide and fragment mass tolerance were set at 0.1 and 0.05 Da, respectively. Only proteins with at least one peptide exceeding their score threshold ($P < 0.05$) and with the molecular weight and p*I* consistent with the gel regions from which the spots were excised, were considered to be positively identified.

### Western blot

SW620 and SW620/irinotecan cells proteins were extracted in radioimmunoprecipitation assay buffer (50 mmol/l tris-base, 1.0 mmol/l EDTA, 150 mmol/l NaCl, 0.1% SDS, 1% Triton X-100, 1% sodium deoxycholate, 1 mmol/l phenylmethylsulfonyl fluoride) and quantified using the DC protein assay kit (Bio-Rad). Samples were separated by 12% SDS-PAGE and transferred to polyvinylidene difluoride membranes (Amersham Biosciences). The membranes were blocked overnight with PBS containing 0.1% Tween 20 in 5% skimmed milk at 4°C, and subsequently probed by the primary antibodies: Rabbit–anti-TDPX1 (diluted 1 : 300, Santa Cruz Biotechnology, USA), α-enolase (diluted 1 : 500; Upstate Biotechnology, Charlottesville, Virginia, USA), or cofilin (diluted 1 : 400; Abcam Massachusetts, USA). Blots were incubated with the respective primary antibodies for 2 h at room temperature and washed three times in tris-buffered saline Tween-20. After that, the blots were incubated with a secondary antibody (diluted 1 : 10 000) conjugated to horseradish peroxidase for 2 h at room temperature. Target proteins were detected using enhanced chemiluminescence reagents (Amersham Pharmacia Biotech, Piscataway, USA). Glyceraldehyde 3-phosphate dehydrogenase was used as an internal loading control.

## Results

### Biological characteristics of SW620/irinotecan cells

The $IC_{50}$ values for irinotecan treatment in SW620 and SW620/irinotecan cells were $3.46 \pm 0.32$ μg/l and $67.3 \pm 9.42$ μg/l, respectively. The resistance of SW620/irinotecan cells to irinotecan was 19.45-fold higher than that of SW620 cells, which meant that the irinotecan-resistant cell line was established successfully.

### Two-dimensional gel electrophoresis profiling of the differentially expressed proteins between SW620 and SW620/irinotecan

The protein expression profiles of SW620 and SW620/irinotecan cells were examined by 2-DE. The experiments were repeated four times. A pair of representative 2-DE maps is shown in Fig. 1. After automatic spot detection, background subtraction, and volume normalization, $653 \pm 18$ protein spots in SW620 cells, and $619 \pm 23$ protein spots in SW620/irinotecan cells were detected.

### Identification of the differentially expressed proteins

Thirty protein spots showed more than two-fold changes in at least three repeats. Among them, 26 spots (86%) were identified by MS (Table 1). The average value of the MOWSE score was 85.6, whereas the average number of unique peptides identified by MS/MS was five. In total, 26 spots were found to be corresponding to the 26 unique proteins, of which, 14 proteins were downregulated in the SW620/irinotecan cells and 12 proteins were upregulated.

### Functional classification analysis

These proteins can be grouped into 16 main functional classes including metabolism (15.38%), cell proliferation/differentiation (11.53%), molecular chaperone (11.53%), mRNA splicing (11.53%), and so on (Fig. 2). One altered

**Fig. 1**

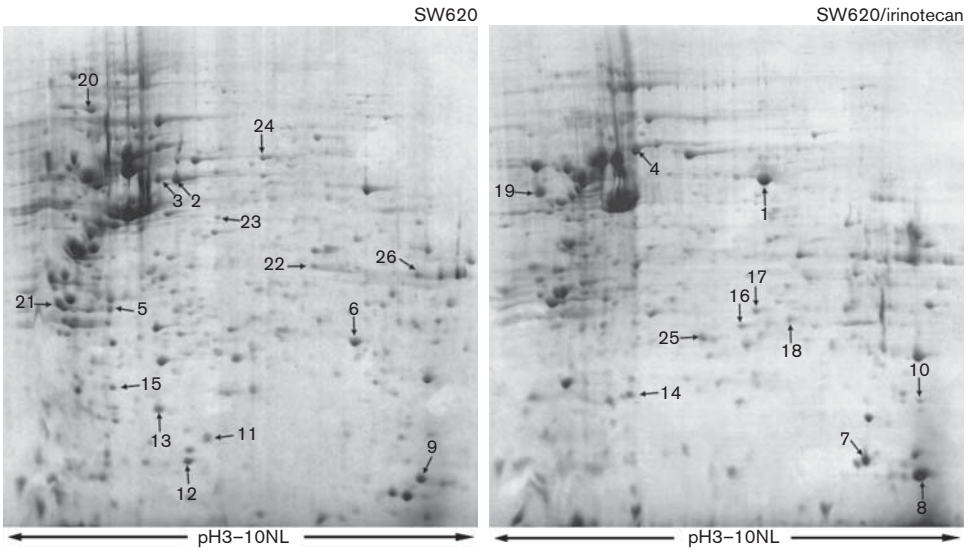


Representative two-dimensional gel electrophoresis gel images of SW620 cells and SW620/irinotecan cells. Total protein extracts were separated on pH 3–10 nonlinear (NL) immobilized pH gradient strips in the first dimension followed by 12% SDS-PAGE in the second dimension, and visualized by coomassie brilliant blue staining. The arrows indicate the 26 differentially expressed proteins.

**Table 1 Identified proteins by MS/MS analysis**

| Spot No. | Protein description | Gene name | Function | Accession No. | Theoretical Mr/pI | Score | No. of peptides | Fold change |
|---|---|---|---|---|---|---|---|---|
| 1 | α-enolase | *ENO1* | Metabolism | P06733 | 47169/6.99 | 99 | 1 | ↑13.7 ± 2.8 |
| 2 | Keratin, type II cytoskeletal 7 | *KRT7* | Cell proliferation/differentiation | P08729 | 51405/5.42 | 87 | 2 | ↓5.7 ± 1.3 |
| 3 | Keratin, type II cytoskeletal 8 | *KRT8* | Structural component | P05787 | 53704/5.52 | 220 | 5 | ↓5.0 ± 1.4 |
| 4 | 60 kDa heat shock protein, mitochondrial | *HSPD1* | Molecular chaperone | P10809 | 61055/5.24 | 106 | 2 | ↑2.9 ± 0.8 |
| 5 | Chloride intracellular channel protein 1 | *CLIC1* | Exocytosis | O00299 | 26923/5.09 | 39 | 2 | ↓4.0 ± 1.7 |
| 6 | Triosephosphate isomerase | *TPI1* | Metabolism | P60174 | 26669/6.51 | 79 | 2 | ↓3.5 ± 1.1 |
| 7 | Nucleoside diphosphate kinase B | *NME2* | Antiapoptosis | P22392 | 17298/8.55 | 118 | 4 | ↑N/A |
| 8 | Peptidyl-prolyl cis-trans isomerase A | *PPIA* | Metabolism | P62937 | 18012/7.82 | 64 | 3 | ↑3.2 ± 0.8 |
| 9 | Cofilin | *COF1* | Cell proliferation/differentiation | Q5KJM6 | 15738/5.55 | 131 | 3 | ↓4.7 ± 2.1 |
| 10 | Transgelin-2 | *TAGLN2* | Metabolism | P37802 | 22319/8.45 | 88 | 4 | ↑N/A |
| 11 | Nucleoside diphosphate kinase A | *NME1* | Cell proliferation/differentiation | P15531 | 17149/5.84 | 74 | 3 | ↓3.6 ± 2.2 |
| 12 | Stathmin | *STMN1* | Signal transduction | P16949 | 17303/5.77 | 64 | 1 | ↓2.4 ± 0.9 |
| 13 | Peroxiredoxin-2 | *PRDX2* | Electron transport/redox regulation | P32119 | 21892/5.67 | 204 | 3 | ↓3.1 ± 1.3 |
| 14 | Phosphatidylethanolamine-binding protein 1 | *PEBP1* | Serine protease inhibitor | P30086 | 21057/5.43 | 44 | 1 | ↑2.7 ± 0.3 |
| 15 | Chromobox protein homolog 3 | *CBX3* | Transcription regulation | Q13185 | 20811/5.23 | 45 | 1 | ↓2.0 ± 0.5 |
| 16 | Peroxiredoxin-4 | *PRDX4* | The activation of NF-kappa-B | Q13162 | 30540/6.54 | 91 | 2 | ↑N/A |
| 17 | Endoplasmic reticulum resident protein 29 | *ERP29* | Protein disulfide isomerase activity | P30040 | 28993/6.08 | 34 | 1 | ↑3.2 ± 1.3 |
| 18 | Proteasome subunit α type-6 | *PSMA6* | Proteolysis | P60900 | 27399/6.35 | 109 | 3 | ↑2.9 ± 1.3 |
| 19 | Calumenin | *CALU* | Calcium ion binding | O43852 | 37107/4.46 | 35 | 1 | ↑2.4 ± 1.0 |
| 20 | 78 kDa glucose-regulated protein | *HSPA5* | Molecular chaperone | P11021 | 72333/5.01 | 99 | 2 | ↓2.6 ± 0.7 |
| 21 | Complement component 1 Q subcomponent | *C1QBP* | Not determined | Q07021 | 31362/4.32 | 38 | 1 | ↓3.1 ± 1.3 |
| 22 | Heterogeneous nuclear ribonucleoprotein H3 | *HNRNPH3* | mRNA splicing | P31942 | 36926/6.37 | 72 | 1 | ↓2.0 ± 0.5 |
| 23 | TAR DNA-binding protein 43 | *TARDBP* | mRNA splicing | Q13148 | 44740/5.85 | 55 | 1 | ↓2.0 ± 0.7 |
| 24 | T-complex protein 1 subunit β | *CCT2* | Molecular chaperone | P78371 | 57488/6.02 | 69 | 2 | ↓2.3 ± 0.9 |
| 25 | Thioredoxin-dependent peroxide reductase | *TDPX1* | Electron transport/redox regulation | P30048 | 27693/5.77 | 86 | 3 | ↑N/A |
| 26 | Heterogeneous nuclear ribonucleoproteinA2/B1 | *HNRNPA2B1* | mRNA splicing | Q2HJ60 | 36006/8.67 | 66 | 3 | ↑2.5 ± 0.8 |

MS/MS, mass spectroscopy; Mr/pI, molecular weight/isoelectric point; N/A, not applicable.

**Fig. 2**

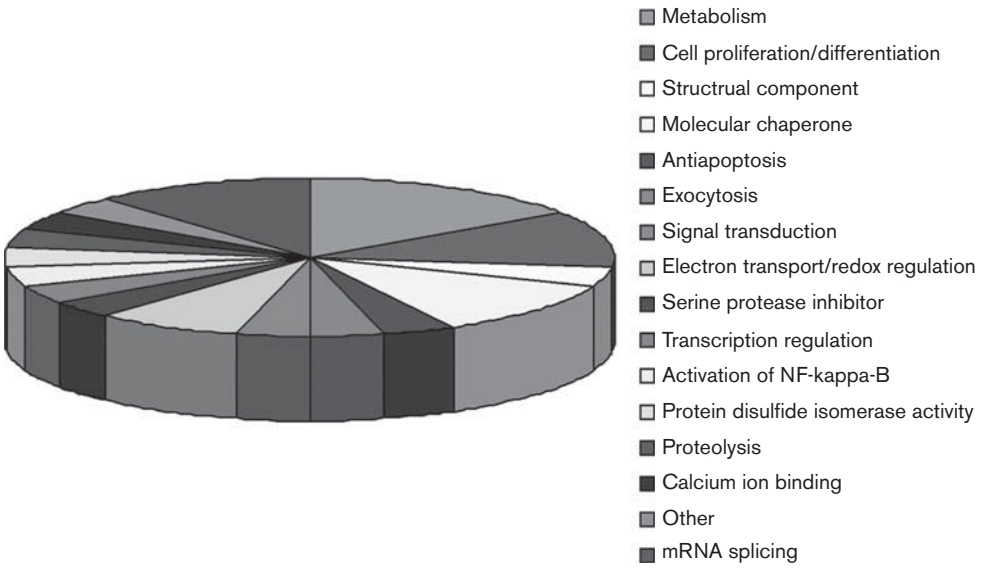


Functional analysis of the 26 identified proteins. These proteins were classified into 16 groups, including metabolism (15.38%), cell proliferation/differentiation (11.53%), molecular chaperone (11.53%), mRNA splicing (11.53%), and so on.

protein, TDPX1, was positively identified with high confidence. The average values of the MOWSE score and the number of unique peptides identified by MS/MS sequencing were 1225.7750 and 3, respectively. A representative MS map of spot #25 is shown in Fig. 3; similar results were obtained according to the MS maps of α-enolase and cofilin (data not shown).

### Protein validation by western blot analysis

TDPX1, α-enolase, and cofilin proteins were further validated by western blot analysis. Consistent with the observations in the 2-DE analysis, TDPX1 and α-enolase were found upregulated and cofilin downregulated in the SW620/irinotecan cells compared with the parental SW620 cells (Fig. 4).

**Fig. 3**

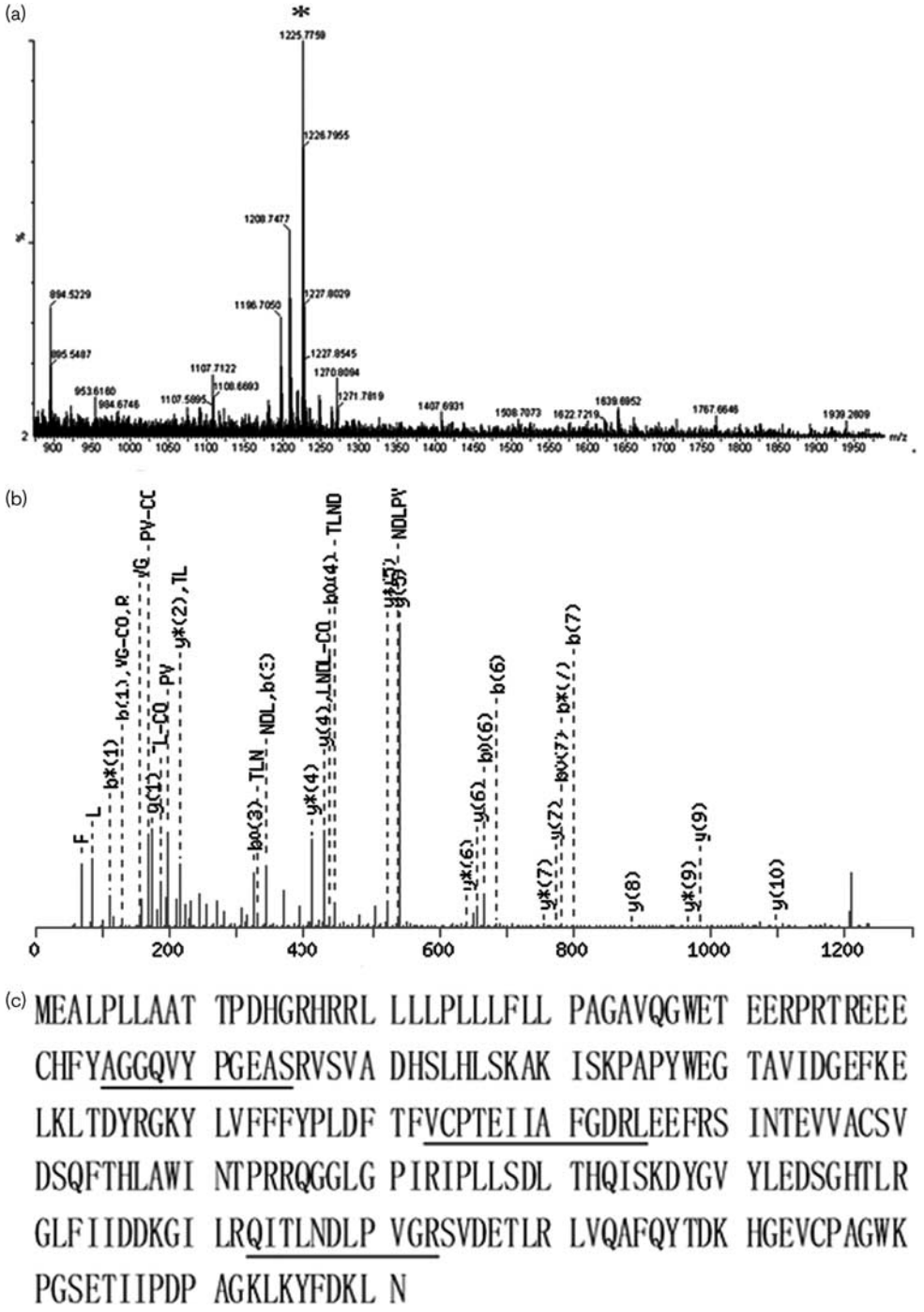


Results of thioredoxin-dependent peroxide 1 (TDPX1) as the representative of protein identification using MALDI-Q-TOF-MS/MS analysis. (a) Mass spectrogram of tryptic peptides from spot #25. (b) An example of a mass spectroscopy (MS/MS) spectrum of the parent ion 1225.7750. (c) Protein sequence of TDPX1. The matched peptides are underlined.

## Discussion

Chemotherapy is a useful tool in prolonged survival and maintaining the quality of life of patients with advanced CRC [3,4]. However, resistance towards anti-cancer drugs develops in approximately one-third of all cases during the treatment [15]. Therefore, identification of the resistance-associated proteins may provide new and specific biomarkers for cancer therapy.

**Fig. 4**

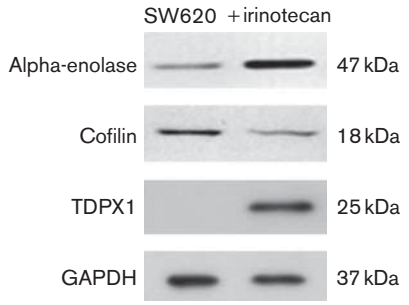


Western blot confirmation of thioredoxin-dependent peroxide 1 (TDPX1), α-enolase, and cofilin corresponding to the spots #25, #1 and #9. As shown, the expression of TDPX1 and α-enolase was upregulated, whereas cofilin expression was downregulated in the SW620/irinotecan cells compared with the SW620 cells. Glyceraldehyde 3-phosphate dehydrogenase (GAPDH) was used as a loading control.

In this study, we established an irinotecan-resistant human colorectal carcinoma cell line SW620/irinotecan. The resistance of SW620/irinotecan to irinotecan was 19.43-fold higher than that of the SW620 cells. The differentially expressed proteins were studied with 2-DE and MS in the SW620/irinotecan cell line compared with its parental cell line SW620. Analyses of biological information showed that some of these proteins were involved in metabolic enzymes, cell proliferation/differentiation, molecular chaperone, mRNA splicing, and so on. Of these proteins, α-enolase, cofilin, and TDPX1 were followed with interest, as they may be associated with the development of tumor drug resistance, as described in earlier studies [16–18].

α-Enolase plays a crucial role in transcription and a variety of pathophysiological processes because of its ability to function as a heat-shock protein and to bind to cytoskletal and chromatin structures [19]. Furthermore, α-enolase was reported to be involved in metastasis through the activation of proenzymes in a proteolytic cascade and selective degradation of matrix components [16]. Overexpression of α-enolase has been reported earlier in cervical [20] and colon [21] cancer cell lines and in breast cancer [22]. This gene product likely reflects the increased glycolysis in cancer cells, which indicate the presence of hypoxia. Hypoxia often contributes to the resistance to chemotherapy or radiotherapy and causes malignant progression. The upregulation of α-enolase in SW620/irinotecan cells in this study suggests that α-enolase might be associated with the mechanism of irinotecan resistance and disease progression.

Cofilin is the actin-severing protein, which is important for the regulation of actin-polymerization initiation and increasing the number of actin-free barbed ends. The underlying mechanisms include: the regulators of actin filament turnover and cytoskeleton reorganization [23,24]; directly responsible for severing actin filaments, regulating actin polymerization, and depolymerization during the cell migration [25]. Reduction of cofilin protein levels with small-interfering RNA resulted in the inhibition of both cytochrome C release and apoptosis [17]. Inhibition of apoptosis is associated with malignancies resistant to chemotherapy. The expression of cofilin was significantly decreased in the SW620/irinotecan cells compared with the SW620 cells in this study, which suggest that resistance to apoptosis may play an important role in the development of acquired irinotecan resistance.

The redox state influences the resistance of the cancer cells to chemotherapy, thus showing an impact in the therapy of the tumor patients [26,27]. One important family of proteins affecting the redox state of the cells is the thioredoxin-dependent peroxide reductase system [28]. The thioredoxin-dependent peroxide reductase encoded by TDPX1 modulates the activity of the thioredoxin system, which plays a major role in removing reactive oxygen species and free radicals [29,30]. Thioredoxin reductase increases oxidant and drug resistance of various cells, and it may be upregulated during drug exposure and be associated with at least cisplatin resistance [18]. Furthermore, this system provides reduced extracellular thioredoxin as a growth factor and it protects the tumor cells from NK-lysin, tumor necrosis factor-α, and from the respiratory burst of immune cells [31,32]. It is, therefore, reasonable to state that tumor cells have been observed to express several fold increased thioredoxin reductase levels [33], and that a number of potent antineoplastic agents such as carmustine, fotemustine, [34,35] and cisplatin [36] are effective inhibitors of mammalian thioredoxin reductase. When considering the tumor-promoting effects of thioredoxin reductase, it is obvious that this selenoenzyme is a major drug target. Elevated expression of thioredoxin might promote cancer cell survival in hypoxic microenvironments of colon carcinomas [34,36]. These findings may help in explaining the results that the upregulated expression of TDPX1 was involved in the development of acquired irinotecan resistance in this study.

### Conclusion

In summary, a total of 26 differentially expressed proteins were identified in the SW620/irinotecan cells, compared with the parental irinotecan-sensitive SW620 cells. The changed expression levels of α-enolase, cofilin, and TDPX1 might be associated with the mechanisms of irinotecan-induced chemoresistance. Further studies are worthy of investigation.

## Acknowledgement

This project was supported in part by National Natural Science Foundation of China (30600550 and 30772538).

## References


1 Greenlee RT, Murray T, Bolden S, Wingo PS. Cancer Statistics, 2000. *CA Cancer J Clin* 2000; **50**:7–33.
2 Jemal A, Siegel R, Ward E, Hao Y, Xu J, Murray T, Thun MJ. Cancer statistics, 2008. *CA Cancer J Clin* 2008; **58**:71–96.
3 Kelly H, Goldberg RM. Systemic therapy for metastatic colorectal cancer: current options, current evidence. *J Clin Oncol* 2005; **23**:4553–4560.
4 Goldberg RM. Therapy for metastatic colorectal cancer. *Oncologist* 2006; **11**:981–987.
5 Rothenberg ML. Irinotecan (CPT-11): recent developments and future directions – colorectal cancer and beyond. *Oncologist* 2001; **6**:66–80.
6 Ark-Otte J, Kedde MA, van der Vijgh WJ, Dingemans AM, Jansen WJ, Pinedo HM, *et al.* Determinants of CPT-11 and SN-38 activities in human lung cancer cells. *Br J Cancer* 1998; **77**:2171–2176.
7 Takahashi T, Fujiwara Y, Yamakido M, Katoh O, Watanabe H, Mackenzie PI. The role of glucuronidation in 7-ethyl-10-hydroxycamptothecin resistance *in vitro*. *Jpn J Cancer Res* 1997; **88**:1211–1217.
8 Loe DW, Deeley RG, Cole SP. Biology of the multidrug resistance associated protein, MRP. *Eur J Cancer* 1996; **32A**:945–957.
9 Liu LF, Desai SD, Li TK, Mao Y, Sun M, Sim SP, *et al.* Mechanism of action of camptothecin. *Ann N Y Acad Sci* 2000; **922**:1–10.
10 Tang G, Minemoto Y, Dibling B, Purcell NH, Li Z, Karin M, Lin A. Inhibition of JNK activation through NF-kappaB target genes. *Nature* 2001; **414**:313–317.
11 Lage H. Proteomics in cancer cell research: an analysis of therapy resistance. *Pathol Res Pract* 2004; **200**:105–117.
12 Righetti PG, Castagna A, Antonioli P, Cecconi D, Campostrini N, Righetti SC. Proteomic approaches for studying chemoresistance in cancer. *Expert Rev Proteomics* 2005; **2**:215–228.
13 Rabilloud T, Adessi C, Giraudel A, Lunardi J. Improvement of the solubilization of proteins in two-dimensional electrophoresis with immobilized pH gradients. *Electrophoresis* 1997; **18**:307–316.
14 Gorg A, Postel W, Weser J, Gunther S, Strahler JR, Hanash SM. Elimination of point streaking on silver-stained two-dimensional gels by addition of iodoacetamide to the equilibration buffer. *Electrophoresis* 1987; **8**:122–124.
15 Hütter G, Sinha P. Proteomics for studying cancer cells and the development of chemoresistance. *Proteomics* 2001; **1**:1233–1248.
16 Pancholi V. Multifunctional α-enolase: its role in diseases. *Cell Mol Life Sci* 2001; **58**:902–920.
17 Pawlak G, Helfman DM. Cytoskeletal changes in cell transformation and tumorigenesis. *Curr Opin Genet Dev* 2001; **11**:41–47.
18 Gilberger TW, Bergmann B, Walter RD, MuËller S. The role of the C-terminus for catalysis of the large thioredoxin reductase from Plasmodium falciparum. *FEBS Lett* 1998; **425**:407–410.
19 Matsuda M, Masutani H, Nakamura H, Miyajima S, Yamauchi A, Yonehara SC, *et al.* Protective activity of adult T cell leukemia-derived factor (ADF) against tumor necrosis factor-dependent cytotoxicity on U937 cells. *J Immunol* 1991; **147**:3837–3841.
20 Elad-Sfadia G, Haklai R, Ballan E, Gabius HJ, Kloog Y. Galectin-1 augments Ras activation and diverts Ras signals to Raf-1 at the expense of phosphoinositide 3-kinase. *J Biol Chem* 2002; **277**:37169–3775.
21 Mialhe A, Louis J, Pasquier D, Rambeaud JJ, Seigneurin D. Expression of three cell adhesion molecules in bladder carcinomas: correlation with pathological features. *Anal Cell Pathol* 1997; **13**:125–136.
22 Pittenger MF, Kazzaz JA, Helfman DM. Functional properties of non-muscle tropomyosin isoforms. *Curr Opin Cell Biol* 1994; **6**:96–104.
23 Ghosh M, Song X, Mouneimne G, Sidani M, Lawrence DS, Condeelis JS. Cofilin promotes actin polymerization and defines the direction of cell motility. *Science* 2004; **304**:743–746.
24 Mouneimne G, Soon L, DesMarais V, Sidani M, Song X, Yip SC, *et al.* Phospholipase C and cofilin are required for carcinoma cell directionality
in response to EGF stimulation. *J Cell Biol* 2004; **166**:697–708.
25 Desmarais V, Ghosh M, Eddy R, Condeelis J. Cofilin takes the lead. *J Cell Sci* 2005; **118**:19–26.
26 Chua BT, Volbracht C, Tan KO, Li R, Yu VC, Li P. Mitochondrial translocation of cofilin is an early step in apoptosis induction. *Nat Cell Biol* 2003; **5**:1083–1089.
27 Tamura T, Stadtman TC. A new selenoprotein from human lung adenocarcinoma cells: purification, properties, and thioredoxin reductase activity. *Proc Natl Acad Sci USA* 1996; **93**:1006–1011.
28 Gladyshev VN, Jeang KT, Stadtman TC. Selenocysteine, identified as the penultimate C-terminal residue in human T-cell thioredoxin reductase, corresponds to TGA in the human placental gene. *Proc Natl Acad Sci USA* 1996; **93**:6146–6151.
29 Sun Y, Oberley LW. Redox regulation of transcriptional activators. *Free Radic Biol Med* 1996; **21**:335–348.
30 Spyrou G, Holmgren A. Deoxyribonucleoside triphosphate pools and growth of glutathione-depleted 3T6 mouse fibroblasts. *Biochem Biophys Res Commun* 1996; **220**:42–46.
31 Andersson M, Holmgren A, Spyrou G. NK-lysin, a disulfide-containing effector peptide of T-lymphocytes, is reduced and inactivated by human thioredoxin reductase. Implication for a protective mechanism against NK-lysin cytotoxicity. *J Biol Chem* 1996; **271**:10116–10120.
32 Mustachich D, Powis G. Thioredoxin reductase. *Biochem J* 2000; **346**:1–8.
33 Arscott LD, Gromer S, Schirmer RH, Becker K, Williams CH Jr. The mechanism of thioredoxin reductase from human placenta is similar to the mechanisms of lipoamide dehydrogenase and glutathione reductase and is distinct from the mechanism of thioredoxin reductase from Escherichia coli. *Proc Natl Acad Sci USA* 1997; **94**:3621–3626.
34 Gromer S, Schirmer RH, Becker K. The 58 kDa mouse selenoprotein is a BCNU-sensitive thioredoxin reductase. *FEBS Lett* 1997; **412**: 318–320.
35 Schallreuter KU, Gleason FK, Wood JM. The mechanism of action of the nitrosourea anti-tumor drugs on thioredoxin reductase, glutathione reductase and ribonucleotide reductase. *Biochim Biophys Acta* 1990; **1054**:14–20.
36 Sasada T, Nakamura H, Ueda S, Sato N, Kitaoka Y, Gon Y, *et al.* Possible involvement of thioredoxin reductase as well as thioredoxin in cellular sensitivity to cis-diamminedichloroplatinum (II). *Free Radic Biol Med* 1999; **27**:504–514.